

Article

Researches on the Macro- and Micro-Structures and Properties of the Vertical Bending Continuous Casted AA6063 Thin Slabs and Their As-Rolled Sheets

Zhuo-Huang Wu, Qi-Jia Mao, Fu-An Hua , Guang-Lin Jia, Jian-Ping Li, Cheng-Gang Li, Guo Yuan and Guo-Dong Wang

State Key Laboratory of Rolling and Automation, Northeastern University, Shenyang 110819, China

* Correspondence: huafa@ral.neu.edu.cn; Tel.: +86-24-83687220

Abstract: A 6063 aluminum alloy thin slab with a cross-section of $260 \times 40 \text{ mm}^2$ was prepared by a vertical bending continuous casting (VC) process. The effects of homogenization, hot rolling and subsequent heat treatments on the microstructure and properties of the as-cast slabs and as-rolled sheets were investigated by scanning electron microscopy (SEM), energy dispersive spectroscopy (EDS), field emission electron probe (EPMA), macro- and micro-structure observation and tensile tests. The results show that the as-cast structure of AA 6063 was dominated by fine and uniform equiaxed grains. After homogenization, all Mg_2Si phases dissolved back, and the Fe-containing intermetallic phases changed from acicular $\beta\text{-Al}_5\text{FeSi}$ phase to spherical $\alpha\text{-Al}_8\text{Fe}_2\text{Si}$ phase. Homogenizing heat treatment before hot rolling can improve the mechanical properties of the alloy. However, in the case of direct rolling without homogenization, the alloy still has good mechanical properties; the strength and plasticity are comparable to that obtained through traditional direct chill (DC) casting, homogenizing and extruding processes, indicating that the VC process has the potential to realize continuous casting and rolling.

Keywords: 6063 aluminum alloy; vertical bending continuous casting; homogenization; hot rolling; microstructure; mechanical properties



Citation: Wu, Z.-H.; Mao, Q.-J.; Hua, F.-A.; Jia, G.-L.; Li, J.-P.; Li, C.-G.; Yuan, G.; Wang, G.-D. Researches on the Macro- and Micro-Structures and Properties of the Vertical Bending Continuous Casted AA6063 Thin Slabs and Their As-Rolled Sheets. *Metals* **2022**, *12*, 1937. <https://doi.org/10.3390/met12111937>

Academic Editor: Andrey Pozdniakov

Received: 18 October 2022

Accepted: 10 November 2022

Published: 12 November 2022

Publisher's Note: MDPI stays neutral with regard to jurisdictional claims in published maps and institutional affiliations.



Copyright: © 2022 by the authors. Licensee MDPI, Basel, Switzerland. This article is an open access article distributed under the terms and conditions of the Creative Commons Attribution (CC BY) license (<https://creativecommons.org/licenses/by/4.0/>).

1. Introduction

There are mainly two methods for the production of aluminum alloy plate, sheet and foil according to the casting process. One is the semi-continuous method (DC) [1,2], that is, the ingot is prepared by the direct chill casting process, and then, the final product is produced from the ingot through sawing, scalping, homogenization, hot rolling, cold rolling, heat treatment, etc. The other is the continuous method (CC) [3–6], that is, the thin strip or slab is cast by twin-roll casting (TRC) or twin-belt continuous casting (TBC), and then is directly hot- or cold-rolled to the final thickness. The advantage of the DC method is that the ingot is thick enough (generally 300 mm–600 mm) after subsequent multi-pass hot rolling, cold rolling and heat treatments, and the mechanical properties and formability of the final products are excellent. In addition, the surface of the final product is also perfect because the scalping eliminates the surface defects of the ingot [7,8]. The DC method is a mature technology, suitable for the production of the full range of aluminum alloys, and is the preferred process for producing high-quality aluminum alloy sheets. However, the DC method also has its shortcomings [8]: (1) It needs to go through a long and complex downstream thermal-mechanical process to produce the final products. (2) The metallic yield is low because the imperfect surface of the ingot needs to be scalped, and the butt of the ingot needs to be sawed off. Meanwhile, fabrication of thin strip or foil from a thick ingot requires many hot and cold rolling passes and heat treatments. All of these processes undoubtedly increase the production cost. (3) The capital investment in the manufacturing facilities is large because it requires not only a lot of thermal-mechanical

processing equipment, but also a deep casting pit and high workshop buildings. The advantages of the CC method are a short technology process route, low capital investment and low production cost [9]. In addition, the microstructures are refined due to the thin thickness of the casting slab (casting strip) and high cooling rate [10]. The disadvantage of this method is that the reduction ratio of the slab (strip) in the subsequent hot or cold rolling process is not enough, and the second phase particles distribute inhomogeneously, so the mechanical properties and formability of the product are inferior to that of the DC method. The surface quality is also difficult to meet class A requirements due to the lack of scalping [11]. Additionally, the CC method is generally only suitable for producing 1xxx, 3xxx and some low Mg content 5xxx alloys. Therefore, its application is limited.

Comparing the characteristics of the DC and CC methods, we find that they seem to show opposite trends in many aspects, such as semi-continuous and continuous casting processes, thick ingot and thin cast strip or slab, strong and weak mechanical properties, good and bad surface quality, high and low production cost and efficiency, etc. This enlightens us on whether there is a process that not only inherits the advantages of the two methods, but also overcomes their shortcomings, so as to achieve a reasonable balance between the above characteristics. The vertical bending continuous casting process (VC) for thin slabs seems to be a promising candidate to meet the abovementioned requirements. The VC process is widely used in the continuous casting of steel ingots [12]. However, to the best of our knowledge, it has not been applied to the continuous casting of aluminum alloys. The VC process has the following features: (1) The solidification process takes place in a water-cooled vertical mold, and then the solidified slab is bent 90 degrees and conveyed out horizontally. In this sense, the VC process is a fully continuous process; therefore, some shortcomings of the DC method, such as frequent cast start-ups and stops, imperfect bottom butts, deep cast pits and explosion risks, etc., are avoided, with the result that high metallic yield, low production cost and capital investment and high safety are realized. (2) The thickness of the slab is between those cast through the DC and CC methods. The VC slab is not as thick as that of DC castings, thus avoiding the long and complex subsequent thermal-mechanical processing, reducing the production cost and investment, and improving the production efficiency. Meanwhile, the slab is thick enough compared to that of CC castings, thus allowing sufficient rolling deformation, which is essential for excellent mechanical properties and formability of the final products. Additionally, the proper slab thickness also makes the material loss caused by slight scalping acceptable; therefore, a surface superior to that obtained by the CC method is possible. (3) The cooling rate of the VC process is higher than that of the DC and TBC processes considering the small ingot thickness and direct water spraying, but lower than that of the TRC process. Although the effects of the cooling rate on microstructure refinement and element segregation may not be as good as those with the TRC process in the CC method, they will be superior to the effects achieved with the DC and TBC processes.

AA6063 belongs to the Al-Mg-Si series of heat-treatable strengthening alloys, and its strengthening phase is mainly due to the Mg_2Si precipitates. Because of its high strength, high corrosion resistance, easy formability and excellent weldability, it is widely used in the architectural and transportation industries [13–17]. The properties of AA6063 are greatly affected by the quantity, size, morphology and distribution of precipitated phases in the ingots [18–21]. Therefore, it is necessary to obtain a good as-cast structure to ensure the properties of the material.

Taking AA6063 as the research object, this study prepared thin slabs by the VC process, then carried out homogenization, hot rolling, solution and aging treatments for the as-cast slabs and the as-rolled sheets. The macro- and microstructures and mechanical properties of the cast slabs and rolled sheets, as well as the influences of the technology processes on the structures and the properties were investigated. The results prove that casting thin aluminum alloy slabs using the VC process is completely feasible, and the mechanical properties of the rolled sheets are comparable or even superior to those cast by the DC method. Further, the feasibility of direct rolling after VC casting was also verified.

2. Materials and Methods

The experimental material was AA6063 with chemical compositions listed in Table 1. Industrial pure Al (99.7%), pure Mg and Al-Si alloy were used as the master alloys for smelting, and the Al-5Ti-1B wires were added into the melt as the refiner.

Table 1. Chemical composition of 6063 alloy (Mass fraction, %).

Element	Mg	Si	Fe	Cu	Ti	Zn	Mn	Cr	Al
Content	0.599	0.417	0.127	0.015	<0.01	0.012	<0.01	<0.01	Bal.

The technological principle and the pilot-scale line of the VC process for thin slab is shown in Figure 1. The VC process mainly includes melting of aluminum alloys, degassing, purification and filtration of the melt, holding of the melt, refinement, solidification in an oscillated and water-cooled mold, pulling-out of the solidified slab, water spray cooling, bending, transferring through an arc segment, straightening, cutting and finally transferring on a horizontal roller table to the downstream process. Specific to this study, about 250 kg of pure Al was melted, and the refinement, slag removal and alloying treatment were carried out in sequence. The pouring temperature was 720 °C, the casting speed was 1.2 m/min, the inner wall of the mold was lubricated with castor oil, and the mold vibrated at a frequency of 150 Hz during the casting process.

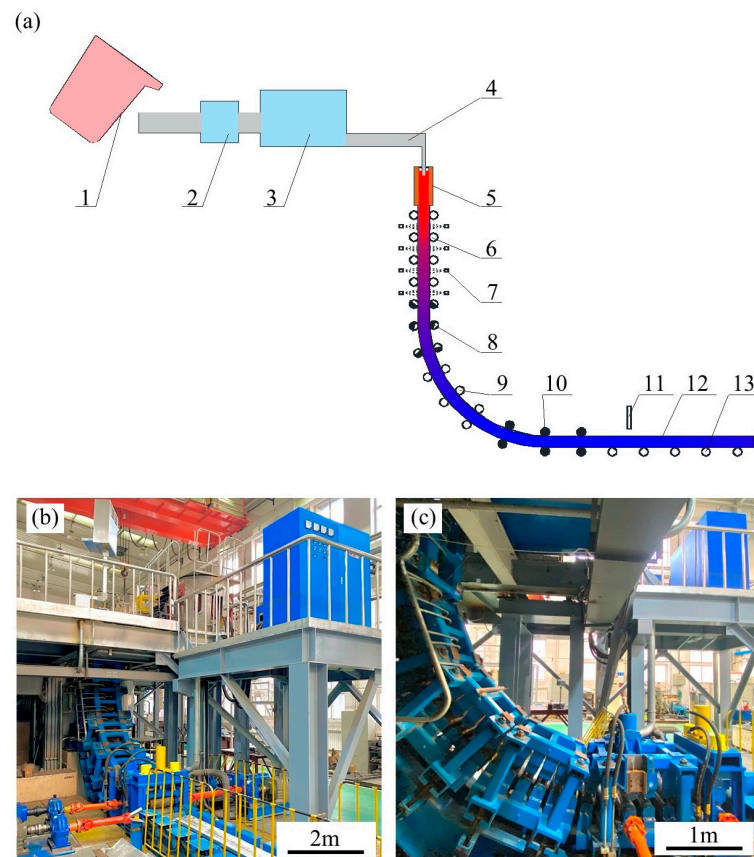


Figure 1. Schematic diagram of principle of the VC process (a) and photos of the pilot-scale line (b) and (c). 1—Melting furnace, 2—Degassing and purification device, 3—Holding furnace, 4—Launder and pouring system, 5—Water cooled mold and oscillating device, 6—Vertical segment rollers, 7—Spray cooling device, 8—Bending segment rollers, 9—Arc segment rollers, 10—Straightening machine, 11—Cutter, 12—Slab, 13—Horizontal roller table.

Homogenization treatment was conducted in a box-type resistance furnace. The slab was homogenized at 570 °C for 10 h and then water-cooled.

The slab was hot-rolled on a 450 mm two-high mill with a roll diameter of $\Phi 450$ mm. The hot rolling process parameters are presented in Table 2.

Table 2. Hot rolling process parameters.

Rolling Temperature	Reduction per Pass	L/h	Rolling Speed	Final Rolled Piece Thickness
480 °C	50%, 45%, 45%, 45%	3.35, 4.09, 5.59, 7.45	0.7 m/s	5 mm

To investigate the effect of slab homogenization on the microstructure and properties of the hot-rolled sheets and explore the feasibility of thin slab continuous casting and rolling based on the VC process, we also rolled the slab without homogenization. The rolled sheets without and with homogenization were named VCR and VHR respectively, and those after solid solution and aging treatments were named VCR-T6 and VHR-T6. The solution treatment of the sheets was carried out at a temperature of 550 °C for 1 h and then water-cooling. The aging treatment parameters were 180 °C, 7 h, and air-cooling.

After casting, the slab was cut transversely and the cross-section was polished with sandpaper and etched for observation of macroscopic morphology. The as-cast specimens for microscopic morphology observation were prepared through mechanical grinding, electrolytic polishing and anodic film coating. The RD-ND section of the rolled sheets was prepared for metallographic observation and analysis. Microstructure observation and phase composition analysis were conducted utilizing a Leica Q550IW image analyzer (Leica Microsystems, Wetzlar, Germany), Zeiss Ultra-55 scanning electron microscope (FEI, Hillsboro, OR, USA), JEOL JXA-8530F field emission electron probe and accompanying energy dispersive spectrometer (JEOL, Tokyo, Japan).

The tensile specimens of the rolled sheets were prepared according to the standard ISO 6892-1: 2019. The gauge length of the specimens was 50 mm. The tensile test was carried out on a WDW-300 microcomputer-controlled electronic universal testing machine (Kexin, Changchun, China) at room temperature. The tensile direction was the rolling direction and the tensile speed was 2 mm/min.

3. Results

3.1. As-Cast Structure of AA6063

Figure 2 shows the AA6063 slab with dimensions of $260 \times 40 \times 6000$ mm³ (width \times thickness \times length) cast by the VC process. The surface of the slab was fairly smooth, without obvious segregation defects and visible surface cracks. The macroscopic structure of the slab is shown in Figure 3. It can be seen that, for the slab of 40 mm thickness, the macrostructure of the whole cross-section was composed of fine and uniform equiaxed grains. This equiaxed grain macrostructure was mainly attributed to the addition of grain refiner and the rapid cooling rate both in the mold and at the stage of water spray cooling.

Figure 4 shows the microstructures at the locations of the outer arc surface, the quarter, the center and the inner arc surface on the cross-section of the slab. Figure 5 shows the metallographic structure at the locations of the center on the cross-section of the slab. It is seen more clearly from Figures 4 and 5 that the as-cast microstructure was dominated by equiaxial dendrites that were α -Al solid solutions and precipitates distributed on the dendrite boundaries. As-cast AA6063 had obvious dendritic segregation, which was caused by the non-equilibrium solidification of the solid solutions under non-equilibrium cooling conditions. In the process of VC solidification, the inner and outer arc surfaces of the slab were cooled rapidly due to direct contact with the mold wall; therefore, the dendrites near the surfaces were fine. With the cooling going on, the solidification front moved towards the core of the slab along the thickness direction, the cooling rate decreased, the dendrite structure became a little coarser, and the secondary dendrites became more developed. The average grain size was measured by the intercept method, and the results are given

in Table 3. Although the grain refinement effect of the VC process is inferior to that of the TRC process [22], it is superior to that of the DC process [23].

EDS composition analysis was carried out for the AA6063 as-cast samples prepared by the VC process. The primary phase morphology is shown in Figure 6. The precipitates of the alloy, including Mg_2Si phase, $\beta-Al_5FeSi$ phase and $\alpha-Al_8Fe_2Si$ phase, were mainly distributed along the grain boundaries. The iron-rich phase was dominated by needle-like $\beta-Al_5FeSi$ phase.

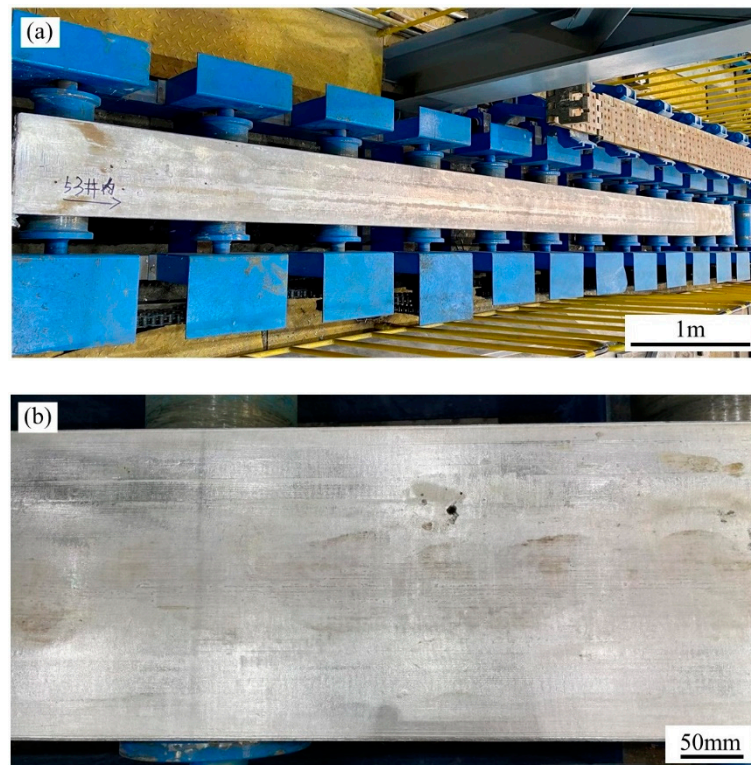


Figure 2. AA6063 thin slab prepared by VC process. (a) Photograph of the whole slab; (b) surface detail.



Figure 3. Macrostructure of as-cast AA6063.

Table 3. Average grain size of VC slab and comparison with other processes. TRC reproduced from [22], with permission from publisher University of Science and Technology Liaoning, 2019. DC reproduced from [23], with permission from publisher J. Mater. Process. Technol, 2004.

Measuring Position	Surface	Quarter	Center	TRC [22]	DC [23]
Grain size/ μm	94 ± 5	95 ± 7	104 ± 1	35	150

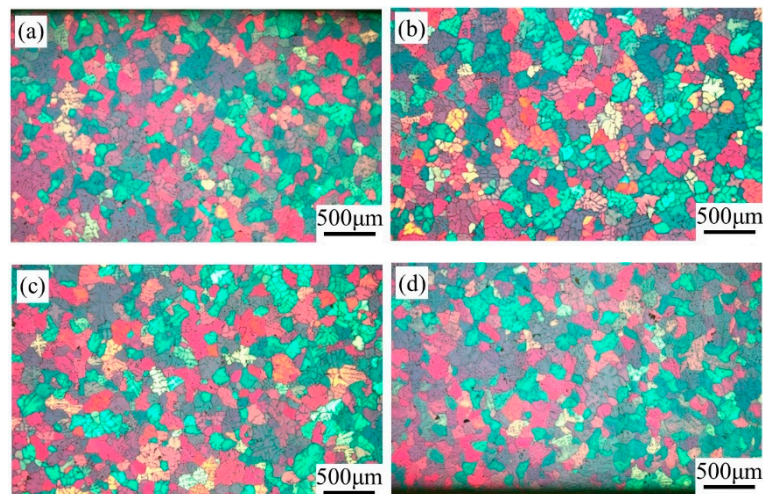


Figure 4. Microstructures of as-cast AA6063 at the locations of (a) outer arc surface, (b) quarter, (c) center and (d) inner arc surface.

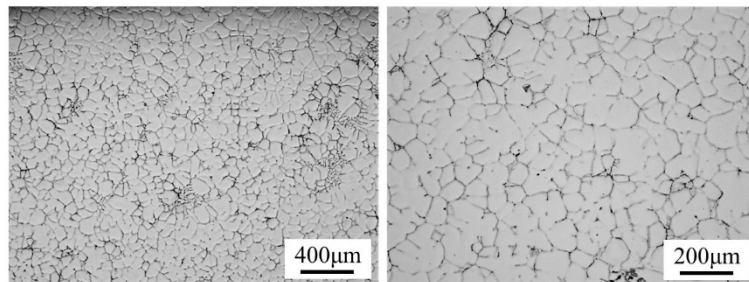


Figure 5. Metallographic structure of as-cast AA6063 at the center locations.

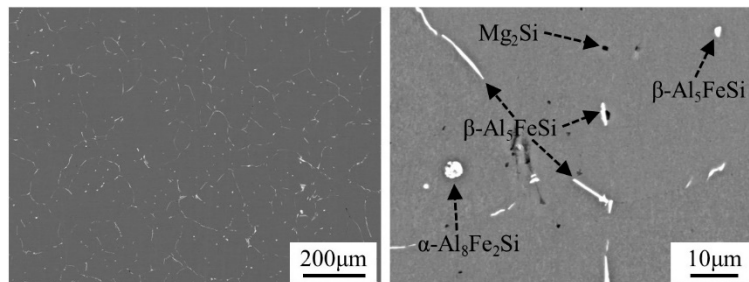


Figure 6. Primary phase morphology of as-cast AA6063.

3.2. Evolution of Precipitates and Alloy Element Distribution

Figure 7 shows an electron backscattering image of the as-cast AA6063 after homogenization treatment. It can be seen that after homogenization, the non-equilibrium eutectic phase dissolved, and the continuous reticular precipitates were broken and distributed discontinuously in the matrix. The results of EDS component analysis of the homogenized samples are presented in Table 4. After homogenization, the white, long, rod-shaped iron-rich phases were transformed into granular or short rod-shaped phases, which were identified as the α - $\text{Al}_3\text{Fe}_2\text{Si}$ phase by energy spectrum analysis.

Figure 8 shows the map scanning results of alloy elements of the as-cast and homogenized specimens. It can be seen from Figure 8 that the solute elements Mg, Si and Fe in the as-cast specimen segregated significantly at the grain boundaries, and the element concentrations gradually decreased from the grain boundary to the interior of the grains. After homogenization treatment, the local concentration of each element decreased and the Mg element distributed uniformly, indicating that the Mg_2Si phase had been completely

dissolved back into the matrix. However, there was still slight segregation of the Si and Fe elements, concentrating in the $\alpha\text{-Al}_8\text{Fe}_2\text{Si}$ phase.

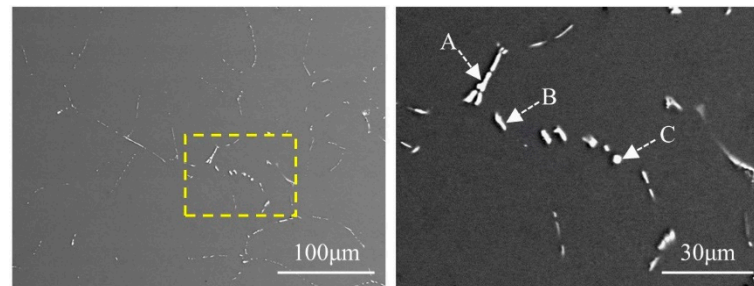


Figure 7. Electron backscattering image of homogenized specimen and energy spectrum dotting position of Table 4.

Table 4. Energy spectrum analysis results of precipitated phase (atomic fraction/%).

EDS Point	Elements		
	Al	Si	Fe
Point A	80.98	6.41	12.61
Point B	86.06	4.22	9.72
Point C	83.51	6.09	10.39

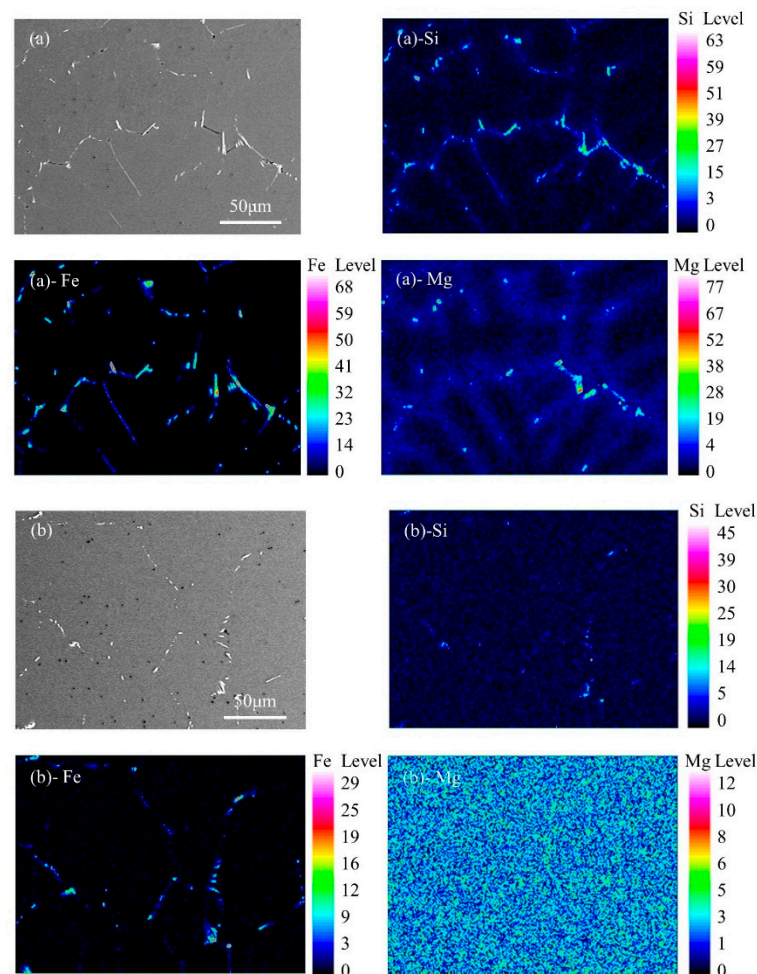


Figure 8. Distribution of solute elements in the specimens. (a) As cast; (b) homogenized.

Figure 9 shows the metallographic structure of VCR and VHR specimens. After hot rolling, the equiaxed grains were elongated into fibrous structures along the rolling direction, and the grain boundaries were blurred. During the hot rolling process, the alloy produced obvious rolling deformation. With the increase in deformation, the proportion of the crystallographic orientation of the grains toward the loading axis increased [24]. Figure 10 shows the morphology and distribution of the precipitated phase of VCR and VHR specimens. After hot rolling, the precipitated phase of AA6063 was crushed and refined under the action of rolling force. The size of the precipitates decreased and their distribution presented a lamellar structure along the rolling direction. For the VCR specimen, the primary Mg_2Si phase was still retained in the matrix, and the iron-rich $\beta-Al_5FeSi$ phase remained unchanged. For the VHR specimen, compared with the VCR specimen, the precipitated phase was smaller in size, rounder in shape, and more evenly distributed, with $\alpha-Al_8Fe_2Si$ as the main component.

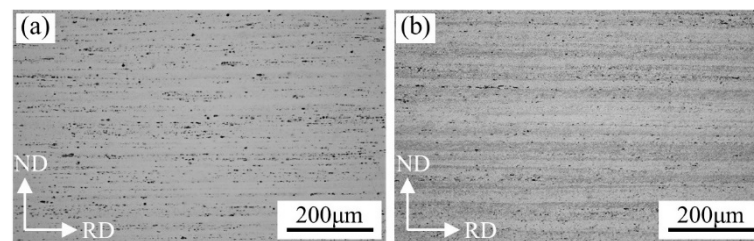


Figure 9. Metallographic structure of hot-rolled 6063 aluminum alloy. (a) VCR; (b) VHR.

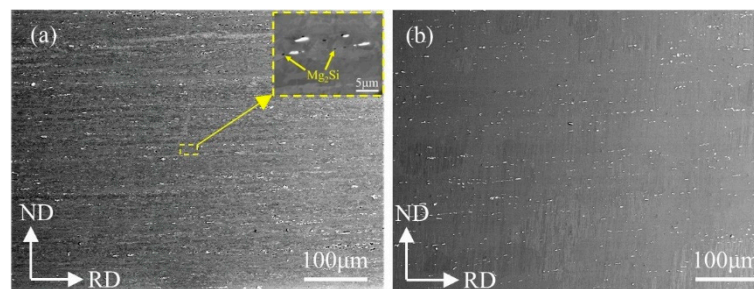


Figure 10. Precipitation morphology and distribution of hot-rolled 6063 aluminum alloy. (a) VCR; (b) VHR.

The map scanning analysis was carried out for the VCR and VHR samples, and the results are shown in Figures 11 and 12. The element distribution in the VCR samples maintained the characteristics of as-cast solidification segregation. Mg, Si and Fe elements were unevenly distributed in the matrix, mainly segregated in the precipitated phase. The solid solution degree of Mg and Si elements in the matrix of the VHR sample were significantly higher than that of the VCR sample, and the distribution of Mg and Si elements in the matrix was more uniform. Because the primary Mg_2Si phase in the VHR sample was completely dissolved into the matrix during the prolonged high-temperature homogenization heat treatment, the high local concentration of Mg element in some areas may have been caused by the re-precipitation of the Mg_2Si phase during the hot rolling process.

Figure 13 shows the hardness of the VCR and VHR rolled sheets. It can be seen that the hardness of the VCR sample was slightly lower than that of the VHR sample, but the difference was not significant. After solution and aging treatment, the hardness of the VHR samples increased by 94%, while the increase in the VCR samples was a little less, just by 72%. Figure 14 shows the tensile properties of the VCR-T6 and VHR-T6 samples. For comparison, the typical tensile properties of AA6063 produced by the DC casting, extruding and T6 heat treatment processes (DCE-T6) [25] are also presented in Figure 14. Compared with VHR-T6, the yield strength and tensile strength of VCR-T6 were slightly lower, but the elongation was almost the same. Compared with the DCE-T6 sample, which

was in a T6 state that had undergone homogenization, solid solution and aging treatment, the VCR-T6 sample had the same mechanical properties.

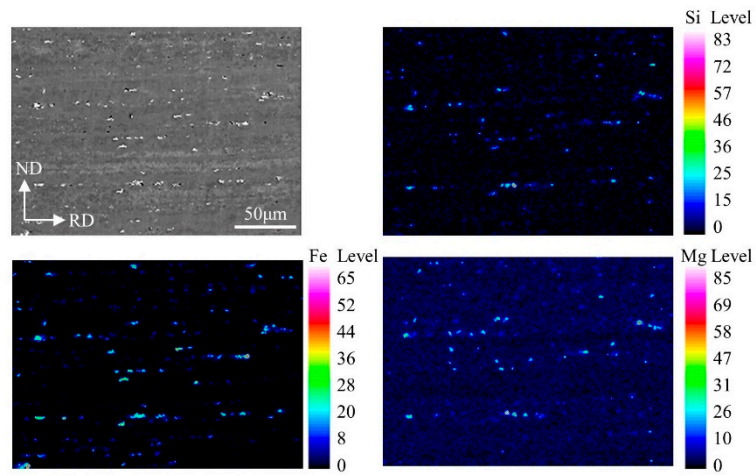


Figure 11. SEM image of alloy element distribution in VCR sample.

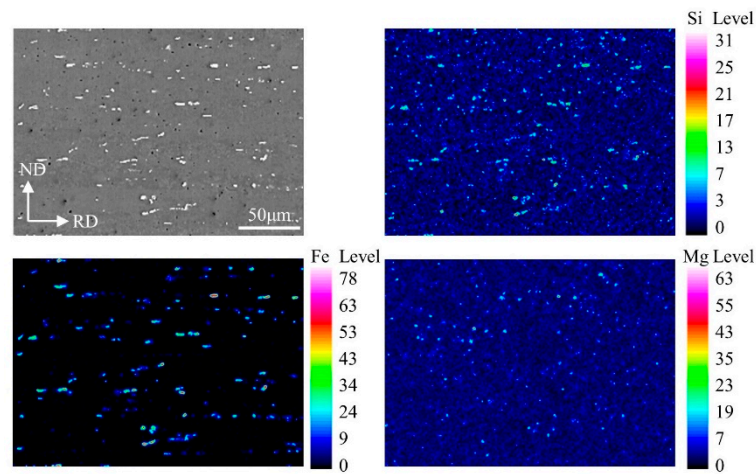


Figure 12. SEM image of alloy element distribution in VHR sample.

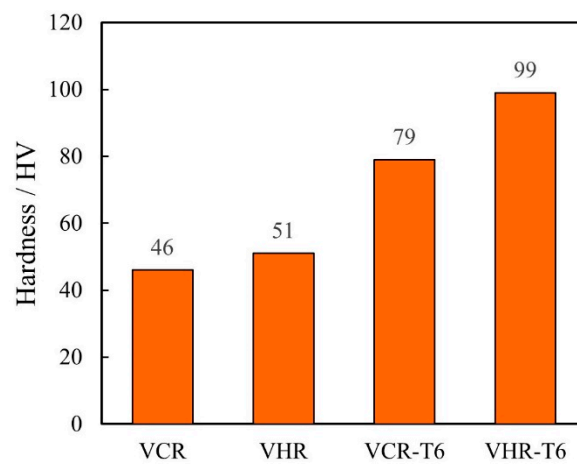


Figure 13. Comparison of hardness values.

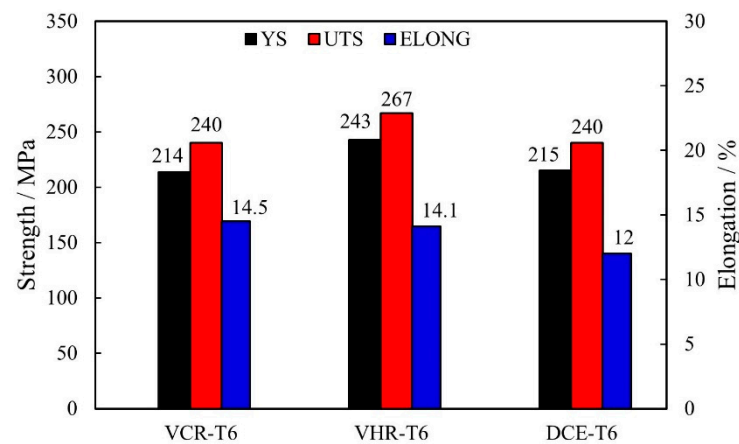


Figure 14. Comparison of tensile properties.

4. Discussion

For AA6063 aluminum alloy, the microstructure of the billet and morphology and distribution of the precipitated phase greatly affect its mechanical properties. Therefore, the billet prepared by the traditional DC casting process needed to undergo a prolonged homogenization heat treatment to improve the severe segregation. Homogenizing heat treatment can make the coarse second phase of segregation in the billet completely dissolve or transform, eliminate the adverse effects of the coarse Mg_2Si phase and hard $\beta-Al_5FeSi$ phase, form a supersaturated solid solution, and precipitate some fine dispersed strengthened phases, so as to improve the mechanical properties of the material. The results of this paper show that AA6063 aluminum alloy can be fabricated by the VC process and directly rolled without homogenizing heat treatment to obtain improved mechanical properties. On the one hand, the billet had a high cooling rate during the whole solidification process due to the direct water spray and relatively small thickness of the slabs, and finally formed a structure completely composed of equiaxed grains, which gave the billet uniform mechanical properties. On the other hand, rapid cooling reduced the dendrite spacing and precipitated phase size of the billet and improved the solution degree of the alloy elements. The small dendrite spacing was beneficial to improve the uniformity of alloying elements in the casting billet, and the uniform distribution of high solid solution structure was beneficial to the uniform and dispersed precipitation of the strengthened phase during the aging process. All of these factors are conducive to improving the mechanical properties of the product. A sufficiently large cooling rate has a positive effect on the element uniformity of the billet, which is similar to the partial effect of homogenization heat treatment, such that the casting billet prepared by the VC process has a certain advantage in mechanical properties, which is also consistent with the test results for the mechanical properties of VCR-T6 and DCE-T6 samples.

The morphology and distribution of the second phase in the as-cast alloy had genetic effects on the properties of the subsequent processing and the final product [26,27]. Compared with the traditional DC casting process, the VC process provides the continuous casting billet with smaller grain size and more uniform structure, which means a product with similar performance can be obtained even if the subsequent processing process is simplified, and provides the possibility for the realization of continuous casting and rolling.

5. Conclusions

In this paper, the macro- and micro-structures of AA6063 thin slabs prepared by the VC process were studied, and homogenization, rolling, solid solution and aging treatments were applied to the as-cast slabs and rolled sheets. The main conclusions are as follows.

- (1) The as-cast structure of AA6063 prepared by the VC process is completely composed of fine and uniform equiaxed grains. There is obvious dendrite segregation, and the

- precipitated phases, including Mg_2Si , $\beta-Al_5FeSi$ and $\alpha-Al_8Fe_2Si$, mainly distribute along the grain boundaries. The iron-rich phase is dominated by the $\beta-Al_5FeSi$ phase.
- (2) Dendrite segregation can be relieved by homogenization heat treatment. After homogenization, all of the Mg_2Si phase is dissolved back, and the acicular $\beta-Al_5FeSi$ phase is transformed into the short-rod or granular $\alpha-Al_8Fe_2Si$ phase. Mg element homogeneously distributes in the matrix, and small amounts of Si and Fe elements are segregated in the $\alpha-Al_8Fe_2Si$ phase.
 - (3) Homogenization heat treatment before hot rolling is beneficial to improving the mechanical properties of AA6063 aluminum alloy. However, direct rolling the VC slabs without homogenization also achieves mechanical properties comparable to those obtained through the DC casting and extrusion processes. This means that continuous casting and rolling based on the VC process is feasible.

Author Contributions: Conceptualization, G.-D.W.; methodology, F.-A.H., G.-L.J. and J.-P.L.; validation, Z.-H.W., Q.-J.M. and C.-G.L.; writing—original draft preparation, Z.-H.W.; writing—review and editing, Z.-H.W. and F.-A.H.; project administration, G.Y. All authors have read and agreed to the published version of the manuscript.

Funding: This research is financially supported by the National Key Research and Development Program of China (2017YFB0304100).

Data Availability Statement: Not applicable.

Conflicts of Interest: The authors declare no conflict of interest.

References

1. Stanley, J.T.; Sanders, R.E.J. *Handbook of Aluminum: Alloy Production and Materials Manufacturing*; Marcel Dekker, Inc.: New York, NY, USA, 2003; Volume 2, pp. 319–342.
2. Granger, D.A. Ingot Casting in the Aluminum Industry. *Treatise Mater. Sci. Technol.* **1989**, *31*, 109–135.
3. Barekar, N.S.; Dhindaw, B.K. Twin-Roll Casting of Aluminum Alloys—An Overview. *Mater. Manuf. Process.* **2014**, *29*, 651–661. [[CrossRef](#)]
4. Szczypiorski, W.; Szczypiorski, R. The Mechanical and Metallurgical Characteristics of Twin-Belt Cast Aluminum Strip Using Current Hazelett Technology. In *Essential Readings in Light Metals*; Springer: Cham, Switzerland, 1991; pp. 949–958.
5. Li, B.Q. Producing thin strips by twin-roll casting—Part I: Process aspects and quality issues. *JOM* **1995**, *47*, 29–33. [[CrossRef](#)]
6. Kim, M.-S.; Kim, S.-H.; Kim, H. Deformation-induced center segregation in twin-roll cast high-Mg Al-Mg strips. *Scr. Mater.* **2018**, *152*, 69–73. [[CrossRef](#)]
7. Sanders, R.E., Jr. Continuous Casting for Aluminum Sheet: A Product Perspective. *JOM* **2012**, *64*, 291–301. [[CrossRef](#)]
8. Maistry, S. Selection of Appropriate Production Process is Fundamental Factor to Improve Enterprise Competition in Aluminum Sheet & Strip Market. *Nonferr. Met. Process.* **2009**, *2*, 765–768.
9. Haga, T.; Tkahashi, K.; Ikawaand, M.; Watari, H. Twin roll casting of aluminum alloy strips. *J. Mater. Process. Technol.* **2004**, *153–154*, 42–47. [[CrossRef](#)]
10. Ferreira, I.L.; Moreira, A.; Aviz, J. On an expression for the growth of secondary dendrite arm spacing during non-equilibrium solidification of multicomponent alloys: Validation against ternary aluminum-based alloys. *J. Manuf. Process.* **2018**, *35*, 634. [[CrossRef](#)]
11. Tewari, A.; Vijayalakshmi, S.; Tiwari, S.; Biswas, P.; Kim, S.; Mishra, R.K.; Kubic, R.; Sachdev, A.K. Influence of Microstructure on Uniaxial Strain Localization in AA5754 Aluminum Sheets Produced by Various Processing Routes. *Metall. Mater. Trans. A* **2013**, *44*, 2382–2398. [[CrossRef](#)]
12. Tanaka, H.; Imamura, A.; Nisihara, R. Effect of Vertical Length for Inclusion Removal in Vertical-bending Type Continuous Casting Machine. *Tetsu-to-Hagane* **2009**, *78*, 1464–1471. [[CrossRef](#)]
13. Hirsch, J. Recent development in aluminium for automotive applications. *Trans. Nonferr. Met. Soc. China* **2014**, *24*, 8. [[CrossRef](#)]
14. Panigrahi, S.K.; Jayaganthan, R. Effect of annealing on precipitation, microstructural stability, and mechanical properties of cry rolled Al 6063 alloy. *J. Mater. Sci.* **2010**, *45*, 5624–5636. [[CrossRef](#)]
15. Zhou, J.; Wan, X.; Li, Y. Advanced Aluminum Products and Manufacturing Technologies Applied on Vehicles Presented at the EuroCarBody Conference. *Mater. Today Proc.* **2015**, *2*, 5015–5022. [[CrossRef](#)]
16. Dinaharan, I.; Murugan, N. Dry sliding wear behavior of AA6061/ZrB2 in-situ composite. *Trans. Nonferrous Met. Soc. China* **2012**, *22*, 810–818. [[CrossRef](#)]
17. Liu, Z.-T.; Wang, B.-Y.; Wang, C.; Zha, M.; Liu, G.-J.; Yang, Z.-Z.; Wang, J.-G.; Li, J.-H.; Wang, H.-Y. Microstructure and mechanical properties of Al-Mg-Si alloy fabricated by a short process based on sub-rapid solidification. *J. Mater. Sci. Technol.* **2020**, *41*, 178–186. [[CrossRef](#)]

18. Gavgali, Y. The effect of homogenization treatment on cold deformations of AA 2014 and AA 6063 alloys. *J. Mater. Process. Technol.* **2004**, *147*, 60–64.
19. Cai, M.; Field, D.P.; Lorimer, G.W. A systematic comparison of static and dynamic ageing of two Al-Mg-Si alloys. *Mater. Sci. Eng. A Struct. Mater.* **2004**, *373*, 65–71. [[CrossRef](#)]
20. Kumar, S.; O'Reilly, K.A.Q. Influence of Al grain structure on Fe bearing intermetallic during DC casting of an Al-Mg-Si alloy. *Mater. Charact.* **2016**, *120*, 311–322. [[CrossRef](#)]
21. Karamis, M.B.; Halici, I. The effects of homogenization and recrystallization heat treatments on low-grade cold deformation properties of AA 6063 aluminum alloy. *Mater. Lett.* **2007**, *61*, 944–948. [[CrossRef](#)]
22. Zhao, D. Twin-Roll Casting Process of 6063 Aluminum Alloy Sheet and Its Microstructure and Properties. Master's Thesis, University of Science and Technology Liaoning, Shenyang, China, 2019.
23. Birol, Y. The effect of homogenization practice on the microstructure of AA6063 billets. *J. Mater. Process. Technol.* **2004**, *148*, 250–258. [[CrossRef](#)]
24. Moshtaghi, M.; Safyari, M.; Kuramoto, S.; Hojo, T. Unraveling the effect of dislocations and deformation-induced boundaries on environmental hydrogen embrittlement behavior of a cold-rolled Al-Zn-Mg-Cu alloy. *Int. J. Hydrogen Energy* **2021**, *46*, 8285–8299. [[CrossRef](#)]
25. Polmear, I.; StJohn, D.; Nie, J.F.; Qian, M. *Light Alloys: Metallurgy of the Light Metals*, 5th ed.; Elsevier (Butterworth-Heinemann): Oxford, UK, 2017; pp. 157–263.
26. Hsu, C.; O'Reilly, K.; Cantor, B.; Hamerton, R. Non-equilibrium reactions in 6xxx series Al alloys. *Mater. Sci. Eng. A* **2001**, *304*, 119–124. [[CrossRef](#)]
27. Erdegren, M.; Ullah, M.W.; Carlberg, T. Simulation of surface solidification in direct-chill 6xxx aluminum billets. *IOP Conf. Ser. Mater. Sci. Eng.* **2012**, *27*, 012013. [[CrossRef](#)]